LIMNOLOGY and OCEANOGRAPHY

ASLO

Limnol. Oceanogr. 9999, 2024, 1–17

doi: 10.1002/lno.12604

Nutrient limitation dampens the response of a harmful algae to a marine heatwave in an upwelling system

Alexis D. Fischer [1], **Emilie Houliez** [2], **Brian D. Bill** [3], **Maria T. Kavanaugh** [4], **Simone R. Alin** [5], **Andrew U. Collins** [6], **Raphael M. Kudela** [7], **Stephanie K. Moore** [8*]

[1]University Corporation for Atmospheric Research (Under Contract to Northwest Fisheries Science Center), National Marine Fisheries Service, National Oceanic and Atmospheric Administration, Seattle, Washington, USA
[2]National Marine Fisheries Service (Sponsored by Franco-American Fulbright Commission and Northwest Fisheries Science Center), National Oceanic and Atmospheric Administration, Seattle, Washington, USA
[3]Environmental and Fisheries Science Division, Northwest Fisheries Science Center, National Marine Fisheries Service, National Oceanic and Atmospheric Administration, Seattle, Washington, USA
[4]College of Earth, Ocean, and Atmospheric Sciences, Oregon State University, Corvallis, Oregon, USA
[5]Pacific Marine Environmental Laboratory, National Oceanic and Atmospheric Administration, Seattle, Washington, USA
[6]Cooperative Institute for Climate, Ocean, and Ecosystem Studies, University of Washington, Seattle, Washington, USA
[7]Ocean Sciences Department, University of California Santa Cruz, Santa Cruz, California, USA
[8]Conservation Biology Division, Northwest Fisheries Science Center, National Marine Fisheries Service, National Oceanic and Atmospheric Administration, Seattle, Washington, USA

Abstract

Harmful algal blooms caused by toxin-producing species of the diatom genus *Pseudo-nitzschia* have been linked to anomalously warm ocean conditions in the Northern California Current System. This study compares summertime concentrations of *Pseudo-nitzschia* spp. and the toxin they produce, domoic acid, during a marine heatwave year (2019) and a climatologically neutral year (2021). An Imaging FlowCytobot was installed on a fishery survey vessel alongside environmental sensors to continuously sample phytoplankton and oceanographic parameters. This was paired with targeted manual sample collections for nutrients, chlorophyll, and domoic acid. Accumulations of *Pseudo-nitzschia* spp. were associated with upwelling zones and established hotspot regions: the Juan de Fuca Eddy, Heceta Bank, and Trinidad Head. Overall, however, *Pseudo-nitzschia* spp. and domoic acid concentrations were low during both summers and appear to have been limited by nitrate. Nutrient availability may therefore modulate the response of *Pseudo-nitzschia* spp. to warm anomalies. Comparison of these results with 2015, another marine heatwave year but one that produced record concentrations of *Pseudo-nitzschia* spp. and domoic acid, suggests that the timing of marine heatwave conditions in the nearshore relative to seasonal upwelling plays a key role in determining whether a *Pseudo-nitzschia* spp. harmful algal bloom will occur.

Multi-scale changes in ocean conditions in the northern California Current System (NCC; Cape Mendocino, California to southern British Columbia; Checkley and Barth 2009) have increased concern over the frequency and intensity of harmful algal blooms (HABs). Seasonal upwelling fuels phytoplankton blooms in the nearshore that sustain important fisheries but

*Correspondence: stephanie.moore@noaa.gov

Additional Supporting Information may be found in the online version of this article.

Author Contribution Statement: ADF: Conceptualization; Data curation; Formal analysis; Funding acquisition; Investigation; Methodology; Project administration; Software; Visualization; Writing – original draft preparation; Writing – review and editing. EH: Methodology; Formal analysis; Writing – original draft preparation; Writing – review and editing. BDB: Investigation; Data curation, Writing – original draft preparation; Writing – review and editing. MTK: Data curation; Writing – review and editing. SRA: Investigation; Data curation; Writing – review and editing. AUC: Investigation; Data curation; Writing – review and editing. RMK: Resources; Writing – review and editing. SKM: Conceptualization; Funding acquisition; Investigation; Methodology; Visualization; Writing—original draft preparation; Writing – review and editing

Special Issue: Autonomous Instrumentation and Big Data: New Windows, Knowledge, and Breakthroughs in the Aquatic Sciencs. *Edited by: Yui Takeshita, Heidi Sosik, Dominique Lefevre, Werner Eckert, Kevin C. Rose and Deputy Editors Julia C. Mullarney, Steeve Comeau, and Elisa Schaum.*

can also fuel HABs of the diatom genus *Pseudo-nitzschia* (Trainer et al. 2000; Smith et al. 2018). Many *Pseudo-nitzschia* species can produce the neurotoxin domoic acid (DA), which is transferred through marine food webs. *Pseudo-nitzschia* HABs cause illness and death in marine mammals and seabirds, and amnesic shellfish poisoning in humans (Todd 1993; Lefebvre et al. 2002). While there is no consensus on the universal drivers of *Pseudo-nitzschia* HABs (Anderson et al. 2021), there does appear to be a link to anomalously warm ocean conditions such as El Niño, warm phases of the Pacific Decadal Oscillation, and marine heatwaves in the NCC (McCabe et al. 2016; McKibben et al. 2017). Given that warm anomalies in the NCC are expected to increase in frequency, duration, and intensity due to climate change (Cai et al. 2014; Scannell et al. 2016; Barkhordarian et al. 2022), it is also likely that *Pseudo-nitzschia* HABs will continue to worsen.

The most well-studied example of a *Pseudo-nitzschia* HAB associated with a warm anomaly is the 2015 event that occurred during the 2014–2016 Northeast Pacific marine heatwave (Bond et al. 2015; Di Lorenzo and Mantua 2016). This event set records for levels of DA in Dungeness crabs (*Metacarcinus magister*) and Pacific razor clams (*Siliqua patula*), which resulted in prolonged closures of these fisheries in California, Oregon, and Washington (McCabe et al. 2016). The anomalously warm waters associated with the marine heatwave allowed *Pseudo-nitzschia australis*, a highly toxigenic species, to expand its geographic range northward and grow at faster rates (McCabe et al. 2016). Because of the unique ability of *P. australis* to both rapidly uptake and utilize a variety of nitrogen sources, it was able to outcompete the rest of the phytoplankton community and bloom along the entire West Coast of the United States following the spring transition to upwelling conditions (Cochlan et al. 2008; Kudela et al. 2010; McCabe et al. 2016). Anomalous nutrient stoichiometry during the upwelling season, where nitrogen was available for DA synthesis but silicate was disproportionately limiting, was associated with the unprecedented levels of particulate DA produced by *P. australis* cells (Ryan et al. 2017; but also see Cochlan et al. 2023). To understand whether the 2015 HAB is representative of *Pseudo-nitzschia*'s response to future warm anomalies in the NCC, more instances of warm anomalies need to be investigated. In particular, the interplay between warm anomalies and in situ nutrient availability over large spatial scales will be useful in determining the effects of a changing NCC on *Pseudo-nitzschia* HABs.

Ocean acidification is another intensifying stressor that can interact with nutrient availability to influence *Pseudo-nitzschia* HABs. The NCC already experiences seawater pH and pCO_2 (partial pressure of carbon dioxide) conditions not predicted for surface waters in other regions until the end of the 21st century. This is due to the upwelling of subsurface North Pacific water masses with high pCO_2 levels from the combination of in situ respiration and the uptake of anthropogenic CO_2 (Hauri et al. 2009; Feely et al. 2016). Climate change is anticipated to intensify upwelling-favorable winds in the NCC (Rykaczewski et al. 2015; Pozo Buil et al. 2021), which would enhance the vertical transport of cold, CO_2- and nutrient-rich subsurface water and amplify ocean acidification in the nearshore (Gruber et al. 2012; Capone and Hutchins 2013). Most of our knowledge of the effects of ocean acidification on *Pseudo-nitzschia* growth and DA production comes from controlled laboratory monoculture studies, but these studies have sometimes yielded conflicting results. For example, *Pseudo-nitzschia* growth rates have been shown to both increase (Sun et al. 2011; Tatters et al. 2012) and decrease (Wingert and Cochlan 2021) when cells were nutrient-replete and maintained at high pCO_2 conditions. There is a growing need to evaluate the interactive effects of pCO_2 and nutrient availability on *Pseudo-nitzschia* growth and toxin production in the field.

Together, these studies suggest that the combined effects of increased warm anomalies and ocean acidification will increase the risk of *Pseudo-nitzschia* HABs in the NCC, but that the response will be modulated by nutrient availability. Yet, few datasets exist to explore these relationships in situ. Several factors have likely contributed to this paucity of available data. Nutrient and carbonate chemistry measurements are both labor-intensive and expensive to obtain, and as such, they are rarely collected (and analyzed) alongside *Pseudo-nitzschia* and DA measurements by most monitoring programs. For *Pseudo-nitzschia* observations, sampling capacity is limited by the labor-intensive microscopy methods that are employed by most monitoring programs. Furthermore, paired observations of *Pseudo-nitzschia*, DA, temperature, pCO_2, and nutrients are rarely collected on temporal and spatial scales that are sufficient for identifying relationships in the dynamic upwelling environment of the NCC. Advances in the development and application of autonomous instrumentation are, however, beginning to alleviate these data gaps by making it technically feasible to continuously monitor phytoplankton communities and carbonate chemistry in the marine environment.

The objective of this study was to use snapshot surveys with high spatial resolution to investigate how summertime concentrations of *Pseudo-nitzschia* and DA varied in the NCC between two years: one impacted by a marine heatwave (2019) and the other climatologically neutral (2021). The data collection platform was a fishery survey vessel that conducted transects throughout the entire NCC during both years. An Imaging FlowCytobot (IFCB; Olson and Sosik 2007) was installed to sample phytoplankton from the ship's underway seawater system, where a thermosalinograph and a General Oceanics pCO_2 Measuring System (Pierrot et al. 2009) were already operational. Sensor data were complemented by targeted manual sampling for nutrients, chlorophyll, particulate DA, and *Pseudo-nitzschia* species identification to provide further ecological context. A machine learning image classifier was developed to quantify *Pseudo-nitzschia* and the rest of the NCC's summer phytoplankton assemblage from IFCB data. Comparison between these summer surveys serves as a case

study to gain insight into how *Pseudo-nitzschia* responds to multiple stressors, specifically warm anomalies and ocean acidification, and the role of nutrients in modulating that response across the NCC. Results from the marine heatwave-impacted survey year are also compared to 2015, the year of the massive HAB that was linked to the 2014–2016 Northeast Pacific marine heatwave, to identify similarities and differences in *Pseudo-nitzschia*'s response to these two warm anomalies.

Methods

Study area

The NCC is part of the California Current eastern boundary upwelling system. Along-coast wind stress is primarily responsible for upwelling of nutrients in the spring and summer that fuels the growth of phytoplankton. Relative to the more southerly regions of the California Current, seasonal upwelling in the NCC is weaker and occurs later in the year over a shorter duration (Bograd et al. 2009; Jacox et al. 2018). There are other physio-chemical mechanisms, however, that contribute to the elevated phytoplankton standing stock observed in the region (Hickey and Banas 2008). Numerous submarine canyons enhance the upwelling of nutrient-rich water onto the continental shelf (Connolly and Hickey 2014), and a range of physical features retain phytoplankton on the shelf, including wide shelves, coastlines without large capes, wind intermittency, and density fronts (Small and Menzies 1981; Hickey et al. 2005; Hickey and Banas 2008). In addition, nutrients from riverine input, primarily delivered by the Strait of Juan de Fuca (outlet for the Salish Sea estuary; Davis et al. 2014) and the Columbia River (Chase et al. 2007), contribute to the high rates of primary productivity in the NCC.

Pseudo-nitzschia HABs in the NCC have been associated with three retentive oceanographic features: the Juan de Fuca Eddy, Heceta Bank, and Trinidad Head (Trainer et al. 2009, 2020; Hickey et al. 2013). The Juan de Fuca Eddy forms just off the entrance of the Strait of Juan de Fuca during the summer (Freeland and Denman 1982; MacFadyen et al. 2008). This feature facilitates nutrient inputs to the region through the doming of the nutricline and enhanced cross-shelf advection of outflow from the Strait of Juan de Fuca (MacFadyen et al. 2008). Heceta Bank, located off central Oregon, is a large submarine bank that extends $\sim$50 km offshore between 43.8°N and 44.6°N. A low-velocity zone is located inshore of the bank, resulting in retention of water and accumulation of biomass in surface waters (Barth et al. 2005). Finally, the Trinidad Head region spans two coastal headlands: Cape Mendocino and Cape Blanco (40.4°N–42.8°N). Upwelling is intensified at these coastal headlands, but on their lee sides, retentive eddies can form (Barth et al. 2000). The retentive circulation pattern of this region has been a persistent source of *Pseudo-nitzschia* HABs since 2015 (Trainer et al. 2020; Harvey et al. 2023). The distribution and transport of these HABs can also be affected by the Columbia River plume, which can both retain (Kudela et al. 2010) and mitigate blooms by inhibiting their shoreward advection to coastal beaches where toxic *Pseudo-nitzschia* cells can be ingested by razor clams (Hickey et al. 2005).

Data collection

High spatial resolution phytoplankton and environmental data were collected during the 2019 and 2021 Integrated Ecosystem and Pacific Hake Acoustic Trawl Survey (hereafter, Hake survey) onboard the National Oceanic and Amospheric Adminstration (NOAA Ship *Bell M. Shimada*. The Hake survey occupies 88 transects, spanning the entire US West Coast and provides a fishery-independent estimate of Pacific Hake (*Merluccius productus*) age-structured biomass and distribution, as well as information on critical ecosystem attributes. The survey takes place every other year during the summer months and coincides with a period of high HAB risk in the NCC (Trainer et al. 2009, 2020, Hickey et al. 2013).

Continuous in situ phytoplankton, pCO_2, and sea surface temperature (SST) and sea surface salinity data were autonomously collected by an IFCB, a General Oceanics pCO_2 Measuring System, and a thermosalinograph, respectively, installed on the ship. Sensor measurements were collected in the NCC (40–49°N) from July 9, 2019 to August 19, 2019 and July 26, 2021 to September 22, 2021. All sensors sampled from the scientific seawater supply, which had an intake at 5-m depth, thereby sampling the well-lit surface mixed layer where phytoplankton are typically most abundant. The IFCB sampled at a rate of $\sim$5 mL seawater every 20 min, the pCO_2 Measuring System sampled every 3 min, and the thermosalinograph sampled every 10 s.

Discrete samples were manually collected from the scientific seawater supply to characterize macronutrients, chlorophyll, particulate DA, and *Pseudo-nitzschia* species composition. The macronutrients measured were nitrate + nitrite ($NO_3^- + NO_2^-$; hereafter, "nitrate"), orthophosphate (PO_4^{3-}; hereafter, "phosphate"), and orthosilicic acid ($Si[OH]_4$; hereafter, "silicate"). More discrete samples were collected in 2019 ($n = 166$) than in 2021 ($n = 60$), but the spatial coverage in the nearshore upwelling zone was equivalent. All discrete samples were analyzed for macronutrients, chlorophyll, and particulate DA, but only a subset with elevated concentrations of particulate DA and/or the genus *Pseudo-nitzschia* were analyzed with scanning electron microscopy to determine the species composition. Detailed information regarding continuous sensor data collection and the methods used to analyze discrete samples is available in the Supporting Information.

Contextual indicators of ocean conditions

Time series of indicators of marine heatwaves, upwelling, and river discharge from the Columbia River were examined to provide temporal context for the survey data. Marine heatwave impacts to the survey region were assessed using NOAA's 1/4° Daily Optimum Interpolation Sea Surface

Temperature (OISST). OISST is a long-term climate data record that incorporates observations from different platforms (satellites, ships, buoys, Argo floats) into a regular global grid. OISST data (1982–2022) were used to calculate daily anomalies, and anomalously warm events that last for five or more days with temperatures warmer than the 90th percentile based on a 30-yr historical baseline period were classified as marine heatwaves following the methods of Hobday et al. (2016). OISST anomaly data were matched with the dates and coordinates of the surveys. OISST data were also used by NOAA's California Current Marine Heatwave Tracker tool (https://oceanview.pfeg.noaa.gov/projects/mhw) to identify the percentage of the exclusive economic zone in marine heatwave status according to Hobday et al. (2016). These time-series data were obtained for Washington (46–48°N), Oregon (42–46°N), and Northern California (38–42°N) for 2015 and 2019. Nutrient flux estimates from along-coast wind-driven upwelling were provided by the Biologically Effective Upwelling Transport Index (BEUTI; Jacox et al. 2018), which estimates vertical transport of nitrate into the surface mixed layer. The BEUTI value per 1° latitude was matched with dates and coordinates of the surveys, and the climatological average of those dates (1988–2022) was calculated. BEUTI values were also used to compare upwelling conditions in 2015 and 2019 in Washington (47°N), Oregon (44°N), and Northern California (41°N). Finally, a proxy for nutrient flux from the Columbia River was provided by discharge data from the mouth of the Columbia River (US Geological Survey stream gage #14246900, Port Westward). Discharge during 2019 and 2021 were compared to the seasonal climatology (1990–2022) to evaluate any anomalies.

Data processing and analyses

A random forest machine learning classification model was developed to automate the taxonomic identification of IFCB images. The final classification model included 22 classes that represented the most abundant phytoplankton in the NCC during the summer. Of these, three were *Pseudo-nitzschia* classes with different chain lengths, six were dinoflagellates, one was a silicoflagellate, and the remaining 12 were other diatoms (Supporting Information Table S1). Average precision and sensitivity scores were 0.94 (SE = 0.01) and 0.88 (SE = 0.01), respectively, across all classes. Abundances of cells in each class were determined using the effective volume analyzed by the IFCB. A more detailed description of classifier development is available in the Supporting Information.

Timestamps were used to pair IFCB samples collected every ~ 20 min with latitude and longitude coordinates, sensor data (temperature, salinity, pCO_2), and discrete samples (macronutrients, chlorophyll, particulate DA, *Pseudo-nitzschia* species microscopy). IFCB matchups were exact for temperature and salinity data and lagged by up to 3 min for the pCO_2 data. Because the time interval between discrete sample collections was longer (~ 6–12 h), matches with IFCB samples lagged by up to 10 min.

Paired IFCB-derived *Pseudo-nitzschia* abundance and particulate DA samples were used to calculate DA cell quotas. DA cell quotas are affected by numerous chemical variables, including major limiting nutrients, and can provide information on environmental conditions that promote toxin production. Despite distances of up to 3.8 km between paired samples, the DA cell quotas calculated in this study were within the ranges reported by previous studies on *Pseudo-nitzschia* from the NCC (Supporting Information Fig. S4; Garrison et al. 1992; Ryan et al. 2017; Wingert and Cochlan 2021).

The mean valve width of *Pseudo-nitzschia* cells in each IFCB sample was calculated from IFCB images by extracting the "MinorAxisLength" feature using the *blob* and *features* extraction procedure (v2) from https://github.com/hsosik/ifcb-analysis. These values were converted to real dimensions using an estimated conversion factor of 3.81 pixels μm^{-1} determined from IFCB images of red-fluorescent bead standard (5.7 μm) collected during both Hake surveys. Linear regression analysis was performed to investigate if *Pseudo-nitzschia* cell size influenced particulate DA levels.

Pearson correlation analysis was conducted to evaluate the environmental factors associated with elevated concentrations of *Pseudo-nitzschia* and particulate DA. Pairwise correlations between *Pseudo-nitzschia* and temperature, salinity, and pCO_2 were calculated using the continuous sensor dataset ($n = 2693$), but any correlation involving particulate DA or nutrients used the smaller discrete dataset ($n = 145$) due to the lower sampling frequency of these variables. An index of nutrient limitation was calculated using ecological stoichiometric nutrient ratios for marine diatoms (N : Si : P; 16 : 15 : 1, Brzezinski 1985). These ratios were log-transformed to prevent biases associated with which element was in the denominator (Isles 2020), such that high values of Si : N and P : N indicated nitrate limitation relative to silicate and phosphate, respectively. Pearson correlations were calculated using data collected in 2019, 2021, and both years combined.

Outlying Mean Index analysis (Dolédec et al. 2000) was used to characterize the realized ecological niche of *Pseudo-nitzschia* relative to the 19 other taxa composing most of the phytoplankton community. The realized ecological niche is the set of favorable conditions under which a species survives, grows, reproduces, and can be observed, and can be described with two indices: marginality and tolerance. Species with high marginality occur in less common habitats in the studied region, whereas those with low marginality occur in typical habitats in the region. High tolerance values are associated with taxa occurring in a wide range of environmental conditions (generalist taxa), while low values of tolerance imply that the taxa are distributed across a limited range of environmental conditions (specialist taxa). Outlying Mean Index analysis was conducted using paired phytoplankton, temperature, salinity, and pCO_2 continuous sensor data ($n = 2693$);

more details regarding this analysis are available in the Supporting Information.

Results

Oceanographic conditions

A marine heatwave impacted nearly the entire survey region in 2019, whereas SST conditions were near-normal during the 2021 survey (Fig. 1a,b). On average, SSTs during the survey period were ~2°C warmer in 2019 (15.4°C ± 2.5; Fig. 1c) compared to 2021 (13.2°C ± 2.4; Fig. 1d), with the largest SST anomalies of 3°C or more observed along the coasts of northern Washington (~ 47–48°N) and Oregon (~ 43.5–46°N; Fig. 1a). Thus, 2021 provided a climatologically neutral comparison to the effects of the 2019 marine heatwave on summertime concentrations of *Pseudo-nitzschia* and particulate DA.

Coastal upwelling signatures were observed during both survey years, as evidenced by cooler, saltier, higher pCO_2, and higher nutrient conditions close to shore (Figs. 1, 2). Upwelling was particularly evident between 40°N and 45°N, consistent with that region having the highest BEUTI values each year (Fig. 2h). In general, BEUTI values were within normal seasonal ranges and were similar between survey years. Despite this, in 2019, the nearshore region from 45°N to 48°N had a diminished coastal upwelling signature. Nutrients were below detection limits at many of the stations sampled in this region; 0% and 6% of these stations had detectable phosphate and nitrate in 2019, respectively, in comparison to 32% and 55% in 2021 (values were determined from equivalent sampling stations; Fig. 2).

The Juan de Fuca Eddy and the Columbia River plume were evident in the survey data during both years. The Juan de Fuca Eddy region can be identified by cool temperatures, high pCO_2, and elevated nutrient concentrations off the northern Washington coast during the summer (Figs. 1, 2). The Columbia River plume can be identified by the low-salinity water extending offshore and to the south from the river mouth in northern Oregon (Fig. 1e,f). Discharge from the Columbia River was seasonally low but within the normal range (Supporting Information Fig. S2). Within the river plume, silicate levels were elevated, reaching a maximum concentration of 308 μM in 2019, while nitrate and phosphate were often undetectable (Fig. 2e–g). In contrast, in 2021, the maximum concentration of silicate was an order of magnitude lower (25 μM), while nitrate and phosphate were detected at most stations.

During both years, nitrate was depleted with mean values below 10 μM, but this depletion was pronounced in 2019. Nitrate was detected in only 23% of samples in 2019 compared to 72% of samples in 2021 (values were determined from equivalent sampling stations; Fig. 2a,b). Ecological stoichiometric ratios for marine diatoms (N : Si : P; 16 : 15 : 1) indicated that nitrate concentrations were limiting relative to silicate and phosphate throughout the NCC. Relative to phosphate, nitrate limitation occurred in 93% and 88% of the samples in 2019 and 2021, respectively (Fig. 2a–d). The few samples with phosphate limitation were dispersed throughout Heceta Bank and the Juan de Fuca Eddy region in 2019, whereas they were mostly located south of the Juan de Fuca Eddy along the Washington coast in 2021. Relative to silicate, nitrate limitation occurred in all of the samples in 2019 and occurred in 92% of the 2021 samples; those few silicate-limited samples in 2021 were located in the Trinidad Head region (Fig. 2a,b,e,f).

Patterns of *Pseudo-nitzschia* and particulate DA

Abundances of *Pseudo-nitzschia* during the 2019 and 2021 surveys were quantified from the 2693 IFCB samples, comprising over 2 million images of phytoplankton, using the machine learning classification model (Supporting Information Table S1). *Pseudo-nitzschia* did not comprise a substantial fraction of the fluorescing phytoplankton biomass during 2019 (1%) or 2021 (2%). The fluorescing phytoplankton biomass was primarily composed of other diatoms (2019: 78%, 2021: 86%), followed by dinoflagellates and a tiny fraction of silicoflagellates. The mean phytoplankton standing stock, as indicated by chlorophyll, was ~ 50% lower in 2019 (3.5 ± 4.6 μg L^{-1}) than in 2021 (6.9 ± 8.6 μg L^{-1}; values were determined from equivalent sampling stations; Supporting Information Fig. S3). The highest chlorophyll values were observed along the Oregon coast, especially Heceta Bank, with maximum concentrations of 21 and 42 μg L^{-1} in 2019 and 2021, respectively.

Pseudo-nitzschia and particulate DA were detected at approximately a third of stations during each survey, but at low concentrations (10–10^2 cells mL^{-1}, < 66 pg mL^{-1}) relative to previously reported values in the NCC (10^3–10^4 cells mL^{-1}, > 66 pg mL^{-1}; Trainer et al. 2009; McCabe et al. 2016, McCabe et al. 2023). To facilitate comparisons across the study region, particulate DA (pDA) concentrations will be referred to as low (< 66 pg mL^{-1}), moderate (66 < pDA < 200 pg mL^{-1}), and high (> 200 pg mL^{-1}) according to the criteria used by the Pacific Northwest HAB Bulletin (McCabe et al. 2023). Regions of elevated abundance of the genus *Pseudo-nitzschia* relative to surrounding waters (hereafter, "*Pseudo-nitzschia* patches") were detected by the IFCB in active upwelling regions and in established hotspot sites. Particulate DA was detected within most of these patches, but was not detected at every station where *Pseudo-nitzschia* was observed by the IFCB (Fig. 3a,b).

In 2019, the highest density *Pseudo-nitzschia* patch was observed in the Juan de Fuca Eddy (maximum = 121 cells mL^{-1}), but only a few stations in the eddy region had detectable particulate DA (Fig. 3a,c,e). A lower density *Pseudo-nitzschia* patch (maximum = 69 cells mL^{-1}) was dispersed throughout the Heceta Bank region where SST anomalies from the marine heatwave were highest (Fig. 1a). Nearly half of the stations in this region had detectable levels of particulate DA, of which 16% were either moderate or high values

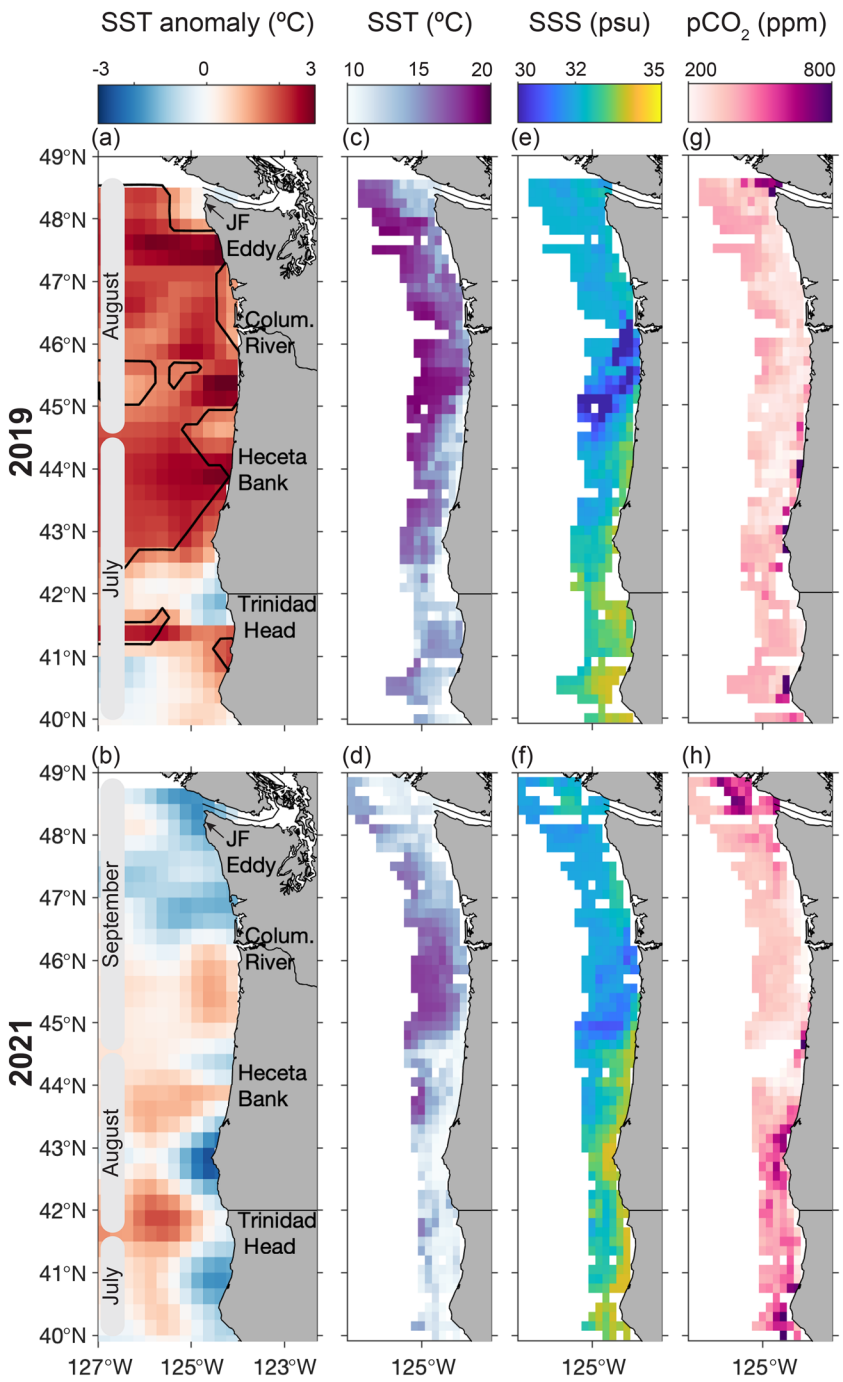

Fig. 1. (**a**, **b**) Sea surface temperature (SST) anomalies with marine heatwave-impacted areas outlined, and continuous sensor observations of (**c**, **d**) SST, (**e**, **f**) sea surface salinity (SSS), and (**g**, **h**) pCO_2 during the 2019 and 2021 Hake surveys. Timing of survey sample collection is shown in shaded boxes on left panels.

(maximum = 216 pg mL^{-1}). During the more normal conditions of summer 2021, the highest density *Pseudo-nitzschia* patches were found in Heceta Bank (maximum = 148 cells mL^{-1}) and the Trinidad Head region (maximum = 154 cells mL^{-1}), but these patches only had low particulate DA levels. A low density *Pseudo-nitzschia* patch was found in the Juan de Fuca Eddy region (maximum = 29 cells mL^{-1}; Fig. 3b,d,f), but this patch had the highest particulate DA concentration measured in this study (maximum = 392 pg mL^{-1}).

Both summers had similar ranges of DA cell quotas (Supporting Information Fig. S1), and regions with high quotas and high particulate DA generally overlapped. For example, the highest DA cell quotas were found in Heceta Bank in 2019 (305 pg $cell^{-1}$) and in the Juan de Fuca Eddy

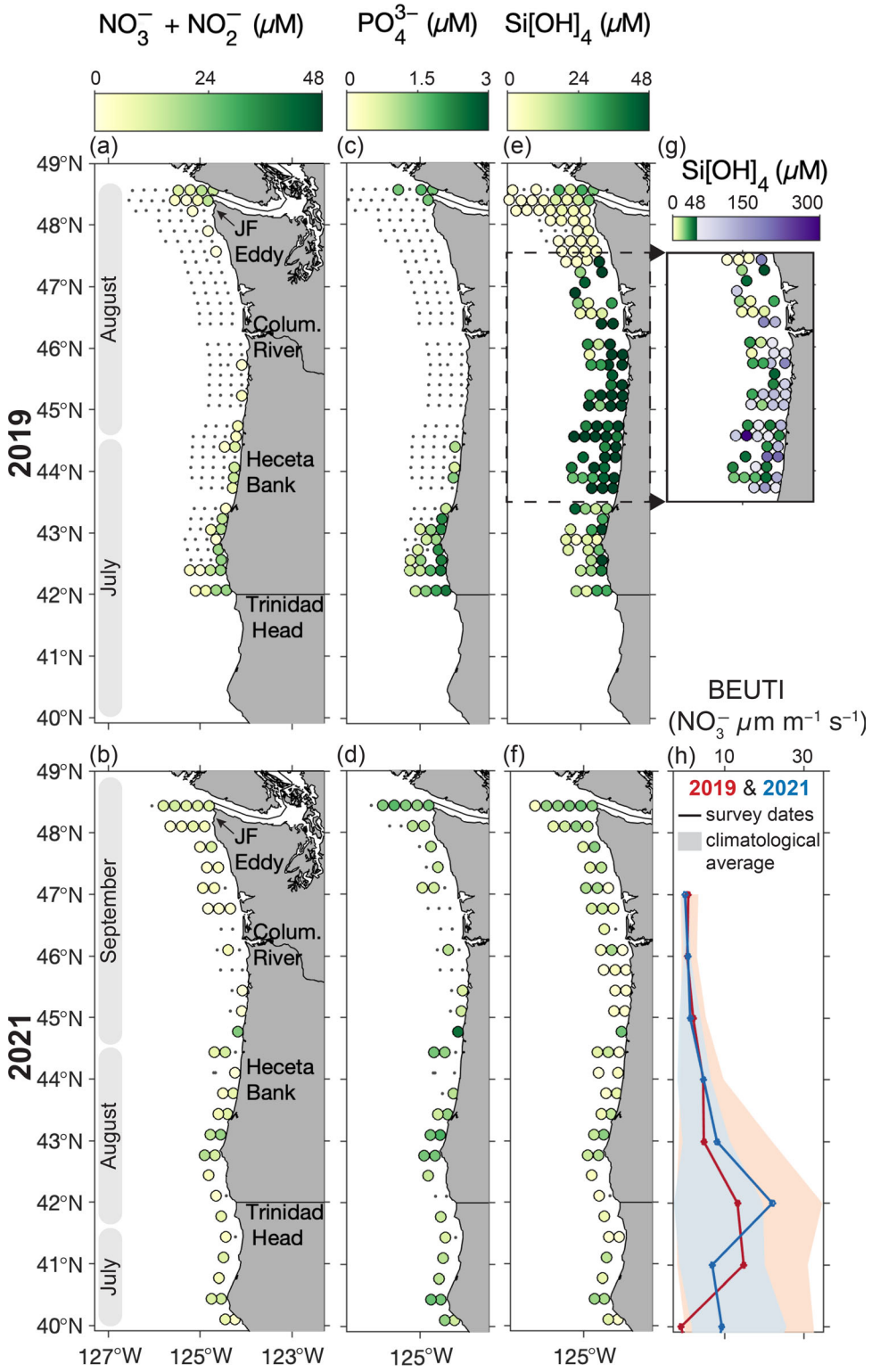

Fig. 2. Surface nutrient concentrations of (**a**, **b**) nitrate + nitrite ($NO_3^- + NO_2^-$), (**c**, **d**) phosphate (PO_4^{3-}), and (**e**, **f**) silicate ($Si[OH]_4$) during the 2019 and 2021 surveys. The maximum color bar ranges reflect stoichiometric relationships among nutrient types for marine diatoms (N : Si : P = 16 : 15 : 1) to clearly indicate regions of nutrient limitation. During 2019, some silicate values exceeded the color bar's scale's maximum within 43.5°N to 47.5°N (dashed box), so panel (**g**) shows the full range of these values. Values below the limit of detection are indicated by the small gray dots. (**h**) Estimates of coastal upwelling-derived nitrate flux are provided by BEUTI at 1° latitude resolution during the survey dates (data were unavailable north of 47°N). The climatological average of BEUTI values for the same dates is shown to provide comparison (1988–2022; shaded areas).

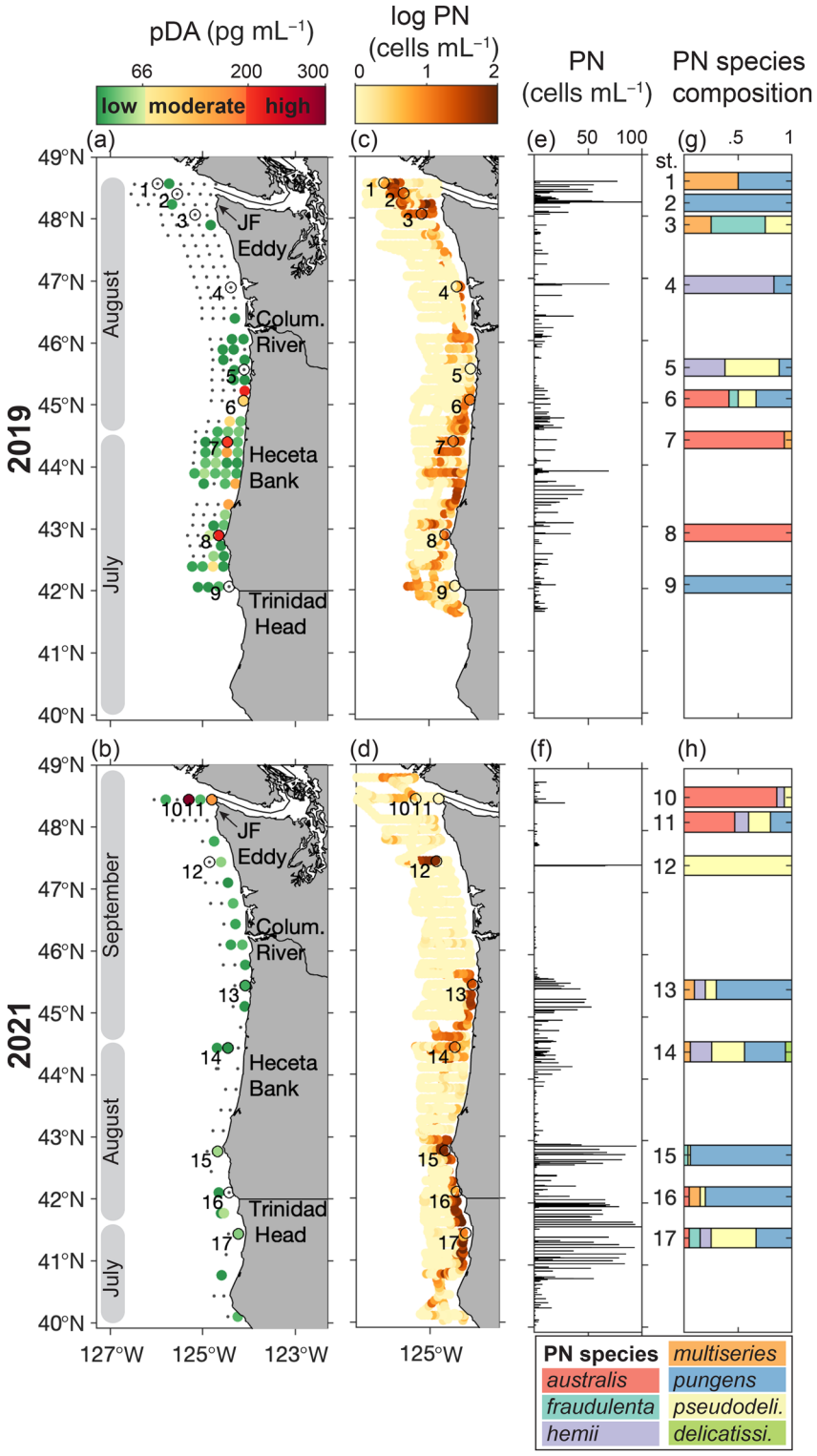

Fig. 3. Particulate DA (pDA) and *Pseudo-nitzschia* (PN) concentrations during the 2019 and 2021 Hake surveys (timing of sample collection is shown in shaded boxes on left panels). (**a**, **b**) Particulate DA concentrations are colored according to the low, moderate, and high toxin risk levels used by the Pacific Northwest HAB Bulletin (McCabe et al. 2023). Sites with values below the detection limit (< 6.4 pg mL^{-1}) are indicated by the small gray dots. IFCB-derived *Pseudo-nitzschia* cell concentration (**c**, **d**) maps and (**e**, **f**) stem plots highlight the spatial extent of *Pseudo-nitzschia* patches and maximum concentrations, respectively. (**g**, **h**) *Pseudo-nitzschia* species composition was determined with scanning electron microscopy at select stations demarcated by numbered circles in (**a**–**d**).

region in 2021 (214 pg cell^{-1}). High DA cell quotas were not significantly driven by low *Pseudo-nitzschia* cell abundances ($R^2 = 0.01$, $F[1, 155] = 1.46$, $p = 0.23$; Supporting Information Fig. S1b), indicating that *Pseudo-nitzschia* patch density was not significantly related to DA cell quotas.

Scanning electron microscopy identified seven species of *Pseudo-nitzschia* that were observed each year: *Pseudo-nitzschia pungens*, *P. australis*, *Pseudo-nitzschia heimii*, *Pseudo-nitzschia pseudodelicatissima*, *Pseudo-nitzschia multiseries*, *Pseudo-nitzschia fraudulenta*, and *Pseudo-nitzschia delicatissima*, ordered from most to least abundant. These taxa have varying sizes and toxin risks (Supporting Information Fig. S5a). A medium-sized species known to have moderate toxin risk, *P. pungens*, dominated the *Pseudo-nitzschia* patches with low particulate DA in the Juan de Fuca Eddy in 2019 (Stas. 1–3), Heceta Bank in 2021 (Stas. 13 and 14), and Trinidad Head in 2021 (Stas. 15–17). One of the largest and most toxigenic species, *P. australis*, dominated both of the *Pseudo-nitzschia* patches with high particulate DA concentrations in Heceta Bank in 2019 (Stas. 6–8) and in the Juan de Fuca Eddy in 2021 (Stas. 10 and 11; Fig. 3g,h). Although *P. australis* was associated with all of the *Pseudo-nitzschia* patches that had high particulate DA in this study, IFCB-derived mean *Pseudo-nitzschia* cell width was not a significant predictor of particulate DA ($R^2 = 0.01$, $F[1, 155] = 1.26$, $p = 0.26$; Supporting Information Fig. S5).

Statistical relationships between *Pseudo-nitzschia* and oceanographic conditions

In 2019, 2021, and both years combined, *Pseudo-nitzschia* had significant negative correlations with temperature and pCO_2, and a significant positive correlation with salinity at $p < 0.01$ (Fig. 4). Yet, the correlation coefficients were considerably stronger for temperature ($r = -0.22$) and salinity ($r = 0.24$), than for pCO_2 ($r = -0.08$). *Pseudo-nitzschia* was generally positively correlated with nutrients and negatively correlated with nitrate limitation relative to silicate and phosphate, but none of these relationships were significant. Particulate DA also had significant negative correlations with temperature in 2019 and both years combined at $p < 0.01$, and had positive correlations with nutrients, several of which were significant at $p < 0.05$ (nitrate in both years, silicate in 2021, phosphate in both years). In general, particulate DA was negatively correlated with nitrate limitation but was significant at $p < 0.05$ on only one instance. Taken together, *Pseudo-nitzschia*'s highly significant correlations with temperature and salinity, and *Pseudo-nitzschia*'s and particulate DA's positive relationships with nutrients (albeit not always significant) were consistent with the *Pseudo-nitzschia* accumulations observed in upwelling zones. *Pseudo-nitzschia*'s and particulate DA's negative correlation with nitrate limitation was also consistent with the nitrate deficit that characterized the surface waters of the NCC during both years.

Outlying Mean Index analysis indicated that the strength of *Pseudo-nitzschia*'s negative relationship with temperature and positive relationship with salinity was comparable to the diatom genera *Thalassiosira*, *Nitzschia*, *Navicula*, *Asterionellopsis*,

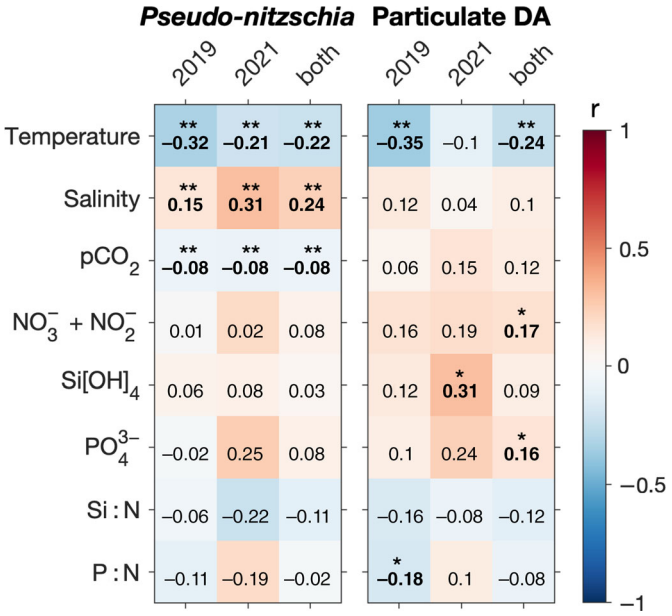

Fig. 4. Pearson correlation heat map showing the relationships between *Pseudo-nitzschia*, particulate DA, and environmental factors for 2019, for 2021, and for both years. Environmental factors include nitrate limitation relative to silicate (Si : N) and relative to silicate (P : N). Correlations between *Pseudo-nitzschia* and sea surface temperature, salinity, and pCO_2 were conducted using the continuous sensor dataset (2019, $n = 1248$; 2021, $n = 1445$; both years, $n = 2693$). All correlations involving particulate DA or nutrients were conducted using the smaller discrete dataset (2019, $n = 97$; 2021, $n = 48$; both years, $n = 145$). Significance at $p < 0.05$ and $p < 0.01$ is indicated by one and two asterisks, respectively.

and *Eucampia* (Supporting Information Fig. S6). The only taxa with a stronger affinity for these conditions was *Dictyocha* spp. None of the phytoplankton taxa had a positive affinity for pCO_2, but *Pseudo-nitzschia* had one of the more neutral affinities. Marginality and tolerance analysis indicated that *Pseudo-nitzschia* was a generalist taxon that occurred over a wide range of the observed NCC conditions but thrived in specific localities within the studied area (i.e., upwelling zones; Supporting Information Fig. S7). Outlying Mean Index analysis results are described in greater detail in the Supporting Information.

Appearance and persistence of marine heatwave conditions in 2015 and 2019

The development of marine heatwave conditions in the coastal zone and upwelling conditions were compared between 2019 and 2015, the year of the massive *Pseudo-nitzschia* HAB that was associated with the 2014–2016 marine heatwave. In 2015, most of the exclusive economic zone from Northern California to Washington was in marine heatwave status throughout the year (Fig. 5, left), with marine heatwave conditions arriving at the coast in September 2014, where they persisted for well over a year (McCabe et al. 2016). As a result, marine heatwave conditions coincided with the onset of the upwelling season. Nutrient influx from upwelling (approximated by

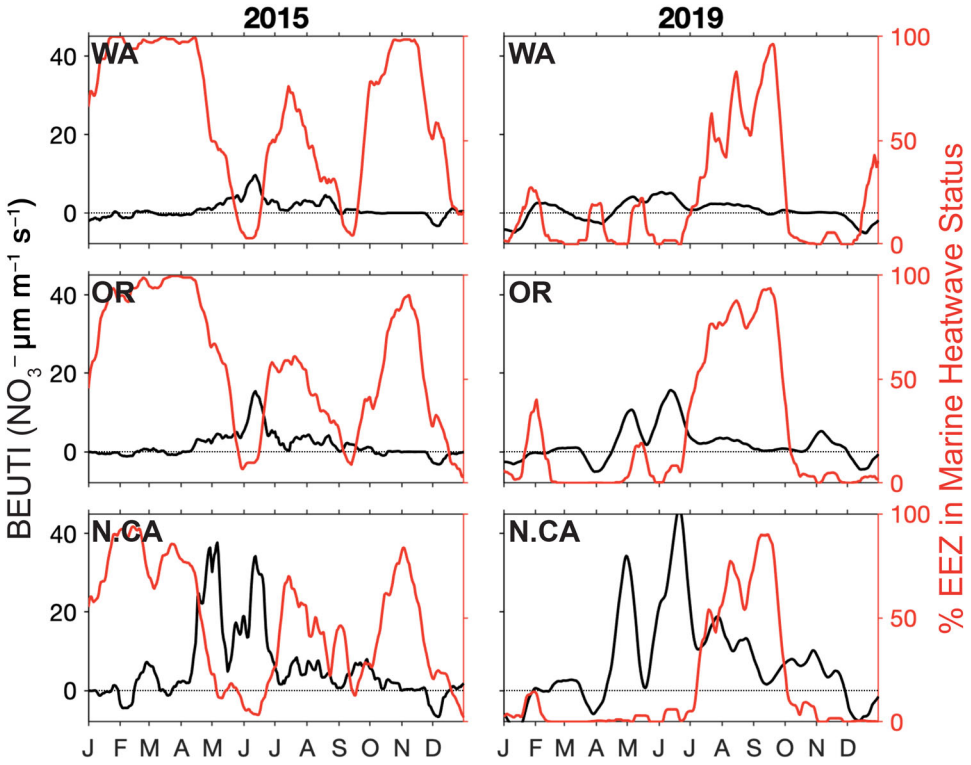

Fig. 5. Timing of coastal upwelling-derived nutrient influx relative to the marine heatwave coverage of the exclusive economic zone (EEZ) in 2015 (left column) and 2019 (right column). Estimates of coastal upwelling-derived nitrate flux in Washington (WA), Oregon (OR), and Northern California (N.CA) are provided by BEUTI at 47°N, 44°N, and 41°N, respectively. The percentage of the EEZ off the coasts of Washington (46–48°N), Oregon (42–46°N), and Northern California (38–42°N) that are in marine heatwave status is shown.

BEUTI) spanned mid-April through October in 2015 in Northern California and was strongest during the first few months following the spring transition. During this time, cold upwelled waters temporarily pushed the marine heatwave offshore, temporarily reducing the percentage of the exclusive economic zone in marine heatwave status (Fig. 5, left). This same general pattern of upwelling-derived nitrate flux occurred in Oregon and Washington waters but was weaker and shifted towards a shorter period. The percentage of the exclusive economic zone in marine heatwave status reached similar values in 2019 as it did in 2015 but appeared for only a ~3-month period that roughly spanned July through September (Fig. 5, right). Furthermore, this timing aligned with the end of the upwelling season, after most of the nutrient influx had already occurred. Any bloom formation would have then been further constrained by the very thin mixed layer that characterized the 2019 marine heatwave (Amaya et al. 2020). As such, there was a mismatch in the appearance of warm anomalies and nutrient availability in nearshore waters in 2019 compared to 2015.

Discussion

Summertime concentrations of *Pseudo-nitzschia* and particulate DA in the NCC were generally low in 2019 and 2021, despite the presence of marine heatwave conditions in 2019. This is in stark contrast to the massive 2015 *Pseudo-nitzschia* HAB, which was associated with the 2014–2016 Northeast Pacific marine heatwave. The absence of any notable accumulations of *Pseudo-nitzschia* and particulate DA appears to be due to a nitrate deficit that characterized the surface waters of the NCC during both summers. The *Pseudo-nitzschia* patches that were observed were associated with upwelled waters and established hotspot regions (i.e., the Juan de Fuca Eddy, Heceta Bank, and Trinidad Head) that are known to be retentive, and harbor relatively higher nutrient concentrations compared to the surrounding waters. Results from this study suggest that nutrient availability can dampen or suppress the response of *Pseudo-nitzschia* to marine heatwaves.

Widespread nitrate depletion may have limited *Pseudo-nitzschia* bloom formation

Several different macronutrients and micronutrients have been observed to limit *Pseudo-nitzschia* bloom formation (e.g., Maldonado et al. 2002), and this study finds strong evidence that nitrate limited *Pseudo-nitzschia* growth during 2019 and 2021. The low nitrate values observed during the summer Hake surveys were also observed by biweekly oceanographic surveys in the coastal waters off central Oregon from July through September (Newport Hydrographic Line; data not

shown), suggesting that these conditions persisted throughout the summer. Nitrogen is essential for the growth of *Pseudo-nitzschia* (and all phytoplankton) and is also required to synthesize DA (Bates et al. 1998). In fact, pulses of nitrogen from upwelling, river runoff after rain events, and resuspended sediments after wind events have all been associated with *Pseudo-nitzschia* blooms in the California Current System (e.g., Wetz and Wheeler 2004; Kudela et al. 2008; Cheng et al. 2021). A lack of nitrate can have the opposite effect on *Pseudo-nitzschia* growth. Previous occurrences of summer nitrate limitation along the Oregon coast have been shown to suppress growth of the phytoplankton community, of which *Pseudo-nitzschia* was a dominant taxon (Frame and Lessard 2009; Kudela and Peterson 2009). While it is apparent that widespread nitrate limitation suppressed *Pseudo-nitzschia* growth during both summer surveys, it is unclear why nitrate depletion in 2019 was so severe.

Enhanced nitrate depletion in 2019 could not be explained by reduced upwelling because BEUTI values (approximating nitrate-flux from wind-driven upwelling) were within normal summer ranges for both surveys (Fig. 2h). Average upwelling also means that enhanced retention of nutrients in the Juan de Fuca Eddy, which would prevent nutrients from leaking from the eddy and being entrained in the southward flowing California Current, cannot explain the nitrate depletion on the Washington coast (MacFadyen et al. 2008). Nor can it be explained by nitrate drawdown from enhanced phytoplankton growth because chlorophyll levels were lower in 2019 compared to 2021 (Supporting Information Fig. S3). One potential explanation is an interaction between upwelling and the marine heatwave. The convergence of cold, nutrient-rich, freshly upwelled waters from the coast with warmer waters from offshore generates SST fronts. At these fronts, density differences can cause upwelled waters to subduct below the warmer waters, thereby reducing the surface expression of nitrate flux (Kadko et al. 1991; Evans et al. 2015). A recent study found that the 2019 marine heatwave constrained an upwelling-induced phytoplankton bloom to Oregon's nearshore zone during the same time as the Hake survey and proposed that water mass density differences reduced cross-shelf transport and enhanced subduction of upwelled waters (Black et al. in press). Enhanced subduction of upwelled waters would be consistent with the strong downward heat fluxes and very shallow mixed layer that characterized the 2019 marine heatwave (Amaya et al. 2020). This proposed mechanism is consistent with the observed narrowing of the upwelling zone (Fig. 1c) and lack of nitrate in surface waters (Fig. 2a) from 45°N to 48°N in 2019, but further investigation is needed to explore this during future marine heatwaves.

A warm anomaly does not necessarily equate to a *Pseudo-nitzschia* HAB

McCabe et al. (2016) reports *Pseudo-nitzschia* and particulate DA concentrations from the 2015 Hake survey, which captured part of the massive HAB that was linked to the 2014–2016 Northeast Pacific marine heatwave. This serves as a comparison for values detected during the 2019 marine heatwave in this study. During the 2015 survey, maximum abundances of *Pseudo-nitzschia* were on the order of 10^3 cells mL^{-1} (McCabe et al. 2016), which is an order of magnitude higher than the maximum abundances observed during the 2019 and 2021 surveys (Fig. 3e,f). Of note, *Pseudo-nitzschia* was quantified using conventional microscopy in 2015, whereas the IFCB was used in 2019, which may have contributed to some differences. An even starker difference, however, is apparent by comparing particulate DA concentrations, which were collected and measured using the same method across years. In 2015, particulate DA reached 4000 pg mL^{-1} (McCabe et al. 2016), but in 2019 it reached only 300 pg mL^{-1} (Fig. 3a,b). Total DA was presumably higher due to contributions from the dissolved pool (Cochlan et al. 2023). Despite the presence of marine heatwave conditions during both the 2015 and 2019 Hake surveys, *Pseudo-nitzschia* and particulate DA values were considerably lower in 2019.

Fishery closure data due to DA contamination were consulted to determine whether the 2019 Hake surveys may have missed any HAB activity outside of the summer snapshot they provided. In contrast to 2015, which had geographically extensive and prolonged fishery closures, there was only one fishery closure in 2019 on the Oregon coast that was due to legacy toxins retained in razor clam tissues from the year before (Harvey et al. 2020). Taken together, the Hake survey and fishery closure data definitively show that despite the presence of marine heatwaves in both 2015 and 2019, a *Pseudo-nitzschia* HAB only occurred in the former year.

This study hypothesizes that the absence of a HAB in 2019 was due to a mismatch in timing of when the marine heatwave made its way to the coast and when ample nutrients from coastal upwelling were available to fuel a bloom in the nearshore surface waters. Both the 2014–2016 and 2019 marine heatwaves produced surface waters in the Northeast Pacific that were 2–3°C warmer than the climatological mean (McCabe et al. 2016; Chen et al. 2021), but those surface waters were also nutrient-depleted. While the warmer waters allow highly toxigenic species like *P. australis* to expand their geographic range northward and enhance growth rates, a *Pseudo-nitzschia* HAB cannot develop without the large input of nutrients from upwelling. The 2019 marine heatwave covered the majority of the NCC's coastal zone from mid-July through September, *after* most of the upwelling-derived nutrient influx had occurred (Fig. 5). In contrast, the 2014–2016 marine heatwave arrived at the coastal zone in the autumn (September 2014), well *before* the 2015 spring upwelling transition, where it persisted for over a year (Fig. 5; McCabe et al. 2016). The overlap of marine heatwave conditions with peak seasonal upwelling in 2015 would have provided replete nutrient conditions for *Pseudo-nitzschia* growth at warm anomaly-enhanced rates, as was observed in Monterey Bay

(McCabe et al. 2016; Ryan et al. 2017). The persistence of the 2014–2016 marine heatwave along the coast also allowed *P. australis* to expand its range northward before the nutrient injection from upwelling (McCabe et al. 2016). These differences in the appearance of marine heatwave conditions in the nearshore relative to upwelling suggest that warm anomalies need to be present before and during the seasonal transition to upwelling conditions for a *Pseudo-nitzschia* HAB to occur.

Complex responses of *Pseudo-nitzschia* growth and toxin production to ocean acidification

Examining the effects of ocean acidification on *Pseudo-nitzschia* is notoriously difficult because increased pCO_2 can benefit carbon acquisition for photosynthesis, while acidified waters can exceed physiological tolerances and cause cellular stress (Beardall and Raven 2004; Hutchins and Fu 2017). Laboratory studies have reported varied responses of *Pseudo-nitzschia* growth and toxin production to ocean acidification and demonstrated that nutrient availability and growth stage can modulate responses (e.g., Lundholm et al. 2004; Tatters et al. 2012; Wingert and Cochlan 2021). It is even more difficult to examine the response of *Pseudo-nitzschia* to ocean acidification in situ, particularly in a dynamic upwelling system like the NCC, due to variations in pCO_2 from both physical and biological processes and interactions with other environmental factors that cannot be controlled.

Pseudo-nitzschia abundance had a significant negative correlation with pCO_2, although it was weak (Fig. 4). In fact, all phytoplankton taxa were found to prefer low pCO_2 conditions (Supporting Information Fig. S6). At first blush, this seems contradictory because both pCO_2 and *Pseudo-nitzschia* were associated with upwelling conditions. Two possible explanations for this result are: (1) high primary production in upwelling regions drawing down CO_2, and (2) insufficient time for *Pseudo-nitzschia* to respond to freshly upwelled water with high pCO_2 in the nearshore. Phytoplankton require CO_2 for photosynthesis, thus low pCO_2 levels in freshly upwelled waters can be indicative of inorganic carbon drawdown due to high primary production (e.g., Evans et al. 2015). Under upwelling conditions, Ekman transport brings nutrient-rich (and high pCO_2) waters to the sunlit surface waters where phytoplankton can utilize them for growth, but also exports phytoplankton offshore (Wilkerson and Dugdale 1987; Mann 2000). This results in a unimodal ("dome-shaped") relationship between upwelling-favorable wind stress and shelf chlorophyll concentrations (Botsford et al. 2003). In the NCC, this chlorophyll curve is shifted towards the shelf side to reflect additional nutrient sources not related to wind stress, such as the Strait of Juan de Fuca and Columbia River (Stone et al. 2020). Indeed, cross-shelf patterns of pCO_2, *Pseudo-nitzschia*, and the phytoplankton community during the 2019 and 2021 Hake surveys are consistent with this dome-shaped relationship. The highest values of pCO_2 were in the nearshore where upwelled waters were freshest, and declined with distance offshore, due to processes such as phytoplankton uptake, outgassing, and mixing (Supporting Information Fig. S4a; Fassbender et al. 2011). Both the highest *Pseudo-nitzschia* abundances and phytoplankton biomass were located between the nearshore and mid-shelf, reflecting the balance of nutrient availability and offshore transport during upwelling (Supporting Information Fig. S4b,c). Particulate DA had a weak positive correlation with pCO_2; however, this relationship was not significant and was largely driven by a small number of high particulate DA values. High pCO_2 has been found to enhance DA production in laboratory studies (Sun et al. 2011; Tatters et al. 2012; Wingert and Cochlan 2021), but such a conclusion cannot be drawn from the field data collected during this study.

Autonomous instrumentation can provide new insights into HABs

The integration of autonomous sensors on the Hake survey generated high spatial resolution data to examine *Pseudo-nitzschia*'s response to environmental stressors over large spatial scales. By leveraging this fishery survey, data were collected for a fraction of the cost that would have been incurred on dedicated oceanographic research cruises. Sensor data identified *Pseudo-nitzschia* patches associated with regional oceanographic features, which were then targeted with discrete samples to identify the species present and the nutrient conditions, as well as which patches were "hot" with particulate DA (or not). This strategic use of a limited number of the more labor-intensive, manually collected, discrete samples further increased efficiency. This paired sampling approach revealed that *P. australis*, a highly toxigenic species, was dominant in the regions with the highest particulate DA concentrations (i.e., Heceta Bank in 2019 and the Juan de Fuca Eddy in 2021). These data also highlighted *Pseudo-nitzschia*'s association with upwelled waters, which has been shown on smaller sub-regional scales in the California Current System (e.g., Trainer et al. 2012; Smith et al. 2018; Sandoval-Belmar et al. 2023). Unlike other studies, however, these high spatial resolution sensor observations revealed that *Pseudo-nitzschia* has one of the highest affinities for upwelling conditions compared to other members of the phytoplankton community (Supporting Information Fig. S6). The consistent spatial footprint of the Hake survey every two years will permit the accumulation of a long-term time series to improve our understanding of *Pseudo-nitzschia*'s response to an NCC increasingly impacted by climate change.

A limitation to pairing autonomous sensor data from the IFCB with discrete samples of particulate DA, nutrients, and *Pseudo-nitzschia* species composition was a mismatch in the timing. The IFCB collected a sample approximately every 20 min, while discrete samples of particulate DA and nutrients were collected at predetermined sites and not always when the IFCB collected a sample. Even though samples were only paired if they were taken less than 10 min apart, this still resulted in mismatches of up to 3.8 km. Due to the spatial heterogeneity of water masses, future sampling from fishery

vessels should strive to collect IFCB and discrete samples from the same station. These paired measurements will greatly improve our ability to confidently draw conclusions regarding the relationship between nutrient limitation, *Pseudo-nitzschia*, and particulate DA in situ.

The snapshot of the NCC captured by the 2019 and 2021 Hake surveys enabled high spatial resolution mapping of the phytoplankton community and important environmental factors over a large geographic domain but lacked high temporal resolution. As such, this study relied on indices of ocean processes, such as BEUTI, to provide temporal context for interpreting results. Pairing high spatial resolution data from mobile observatories, such as the fishery survey vessels in this study, with high temporal resolution data from fixed platforms within the sampling domain is a powerful combination that would better facilitate examination of the mechanisms that lead to *Pseudo-nitzschia* bloom development, as well as HAB monitoring and forecasting. To meet the objective of data production and integration on the appropriate temporal and spatial scales, coordination of HAB observing efforts by multiple entities will be key. In the United States, this high-level coordination is being facilitated by the National HAB Observing Network (Hurst et al. 2020). Furthermore, new insights into HAB dynamics are being revealed through advancement of autonomous sensors. For example, the Environmental Sample Processor is an electromechanical fluidics system that can remotely and autonomously monitor HAB species, DA, and other HAB toxins (Scholin et al. 2009; Doucette et al. 2009; Moore et al. 2021), and more recently has been used to collect and archive samples to examine the expression of toxin biosynthesis genes (Den Uyl et al. 2022; Thukral et al. In press). Some of these sensors are being integrated into uncrewed vehicles (e.g., Tethys-class long-range autonomous underwater vehicles, Saildrones), showing promise for increasing data availability across large spatial areas (Den Uyl et al. 2022; Preston et al. 2024). With a framework to integrate new and existing HAB observing capabilities effectively and efficiently, including the targeted use of advanced autonomous sensors, data at the necessary temporal and spatial scales will increasingly become available to tease apart the effects of multiple stressors on HABs in dynamic environments.

Conclusion

The interacting effects of multiple stressors in a dynamic upwelling system may result in unforeseen changes to *Pseudo-nitzschia* HABs in the NCC. Thus, studies that produce big data on highly resolved spatial and temporal scales are needed to unravel the complexity of *Pseudo-nitzschia*'s response to these changing conditions in situ. This study demonstrates the value of high spatial resolution data collected by autonomous instrumentation installed on fishery survey vessels, showing that widespread nitrate limitation suppressed the development of *Pseudo-nitzschia* HABs during 2019 and 2021, despite the presence of marine heatwave conditions in 2019. Comparison between the conditions observed in 2019 and in 2015, the year of the massive *Pseudo-nitzschia* HAB linked to the 2014–2016 Northeast Pacific marine heatwave, suggests that the timing of warm anomalies in the coastal zone relative to the onset of upwelling conditions may be important for HAB development. This finding highlights the complexity of factors needed to sustain *Pseudo-nitzschia* HABs in upwelling systems, beyond the presence of warm anomalies. This study also provides a glimpse into the power of IFCB data for examining interactions between the genus *Pseudo-nitzschia* and the rest of the phytoplankton community. As IFCB data accumulates in the NCC, the opportunity for rigorously exploring the role of biotic interactions in *Pseudo-nitzschia* bloom development will increase. Future studies coupling autonomous data collection from fixed and mobile platforms on expanded temporal and spatial scales will build upon the data presented here to elucidate the mechanisms behind the response of *Pseudo-nitzschia* to climate stressors in the dynamic NCC system.

Data availability statement

Environmental sensor data that support the findings of this study are openly available from NOAA Fisheries InPort at https://www.fisheries.noaa.gov/inport/item/18471, GUID: gov.noaa.nmfs.inport:18471. Imaging FlowCytobot data and discrete data are available from the corresponding author upon reasonable request.

References

Amaya, D. J., A. J. Miller, S. P. Xie, and Y. Kosaka. 2020. Physical drivers of the summer 2019 North Pacific marine heatwave. Nat. Comm. **11**: 1903. doi:10.1038/s41467-020-15820-w

Anderson, D. M., and others. 2021. Marine harmful algal blooms (HABs) in the United States: History, current status and future trends. Harmful Algae **102**: 101975. doi:10.1016/j.hal.2021.101975

Barkhordarian, A., D. M. Nielsen, and J. Baehr. 2022. Recent marine heatwaves in the North Pacific warming pool can be attributed to rising atmospheric levels of greenhouse gasses. Commun. Earth Environ. **3**: 131. doi:10.1038/s43247-022-00461-2

Barth, J. A., S. D. Pierce, and R. L. Smith. 2000. A separating coastal upwelling jet at Cape Blanco, Oregon and its connection to the California Current System. Deep Sea Res. II Topic Stud. Oceanogr. **47**: 783–810. doi:10.1016/S0967-0645(99)00127-7

Barth, J. A., S. D. Pierce, and R. M. Castelao. 2005. Time-dependent, wind-driven flow over a shallow mid shelf submarine bank. J. Geophys. Res. Oceans **110**: 1–20. doi:10.1029/2004JC002761

Bates, S. S., D. L. Garrison, and R. A. Horner. 1998. Bloom dynamics and physiology of domoic-acid-producing *Pseudo-nitzschia* species, p. 267–292. *In* D. M. Anderson, A. D. Cembella, and G. M. Hallegraeff [eds.], Physiological ecology of harmful algal blooms. NATO ASI Ser. v. **G41**. Springer Verlag.

Black, I., M. T. Kavanaugh, and C. Reimers. in press. Bloom compression by marine heatwaves contemporary with the Oregon upwelling season. Paper presented at Ocean Sciences Meeting, February 20, 2024, New Orleans, LA.

Beardall, J., and J. A. Raven. 2004. The potential effects of global climate change on microalgal photosynthesis, growth and ecology. Phycologia **43**: 26–40. doi:10.2216/i0031-8884-43-1-26.1

Bograd, S. J., I. Schroeder, N. Sarkar, X. Qiu, W. J. Sydeman, and F. B. Schwing. 2009. Phenology of coastal upwelling in the California Current. Geophys. Res. Lett. **36**: 1–5. doi:10.1029/2008GL035933

Bond, N. A., M. F. Cronin, H. Freeland, and N. Mantua. 2015. Causes and impacts of the 2014 warm anomaly in the NE Pacific. Geophys. Res. Lett. **42**: 3414–3420. doi:10.1002/2015GL063306

Botsford, L. W., C. A. Lawrence, E. P. Dever, A. Hastings, and J. Largier. 2003. Wind strength and biological productivity in upwelling systems: An idealized study. Fish. Oceanogr. **12**: 245–259. doi:10.1046/j.1365-2419.2003.00265.x

Brzezinski, M. A. 1985. The Si:C:N ratio of marine diatoms: Interspecific variability and the effect of some environmental variables. J. Phycol. **21**: 347–357. doi:10.1111/j.0022-3646.1985.00347.x

Cai, W., and others. 2014. Increasing frequency of extreme El Niño events due to greenhouse warming. Nat. Clim. Change **4**: 111–116. doi:10.1038/nclimate2100

Capone, D. G., and D. A. Hutchins. 2013. Microbial biogeochemistry of coastal upwelling regimes in a changing ocean. Nat. Geosci. **6**: 711–717. doi:10.1038/ngeo1916

Chase, Z., P. G. Strutton, and B. Hales. 2007. Iron links river runoff and shelf width to phytoplankton biomass along the US West Coast. Geophys. Res. Lett. **34**: 1–4. doi:10.1029/2006GL028069

Checkley, D. M., Jr., and J. A. Barth. 2009. Patterns and processes in the California Current System. Prog. Oceanogr. **83**: 49–64. doi:10.1016/j.pocean.2009.07.028

Chen, Z., J. Shi, Q. Liu, H. Chen, and C. Li. 2021. A persistent and intense marine heatwave in the Northeast Pacific during 2019–2020. Geophys. Res. Lett. **48**: e2021GL093239. doi:10.1029/2021GL093239

Cheng, Y., V. N. Bhoot, K. Kumbier, M. P. Sison-Mangus, J. B. Brown, R. Kudela, and M. E. Newcomer. 2021. A novel random forest approach to revealing interactions and controls on chlorophyll concentration and bacterial communities during coastal phytoplankton blooms. Sci. Rep. **11**: 19944.

Cochlan, W. P., J. Herndon, and R. M. Kudela. 2008. Inorganic and organic nitrogen uptake by the toxigenic diatom *Pseudo-nitzschia australis* (Bacillariophyceae). Harmful Algae **8**: 111–118. doi:10.1016/j.hal.2008.08.008

Cochlan, W. P., B. D. Bill, A. B. Cailipan, and V. L. Trainer. 2023. Domoic acid production by *Pseudo-nitzschia australis*: Re-evaluating the role of macronutrient limitation on toxigenicity. Harmful Algae **125**: 102431. doi:10.1016/j.hal.2023.102431

Connolly, T. P., and B. M. Hickey. 2014. Regional impact of submarine canyons during seasonal upwelling. J. Geophys. Res. Oceans **119**: 953–975. doi:10.1002/2013JC009452

Davis, K. A., and others. 2014. Estuary-enhanced upwelling of marine nutrients fuels coastal productivity in the US Pacific Northwest. J. Geophys. Res. Oceans **119**: 8778–8799. doi:10.1002/2014JC010248

Den Uyl, P. A., and others. 2022. Lake Erie field trials to advance autonomous monitoring of cyanobacterial harmful algal blooms. Front. Mar. Sci. **9**: 1021952. doi:10.3389/fmars.2022.1021952

Di Lorenzo, E., and N. Mantua. 2016. Multi-year persistence of the 2014/15 North Pacific marine heatwave. Nature Clim. Change **6**: 1042–1047. doi:10.1038/nclimate3082

Dolédec, S., D. Chessel, and C. Gimaret-Carpentier. 2000. Niche separation in community analysis: A new method. Ecology **81**: 2914–2927. doi:10.2307/177351

Doucette, G. J., and others. 2009. Remote, subsurface detection of the algal toxin domoic acid onboard the environmental sample processor: Assay development and field trials. Harmful Algae **8**: 880–888. doi:10.1016/j.hal.2009.04.006

Evans, W., B. Hales, P. G. Strutton, R. K. Shearman, and J. A. Barth. 2015. Failure to bloom: Intense upwelling results in negligible phytoplankton response and prolonged CO_2 outgassing over the Oregon shelf. J. Geophys. Res. Oceans **120**: 1446–1461. doi:10.1002/2014JC010580

Fassbender, A. J., C. L. Sabine, R. A. Feely, C. Langdon, and C. W. Mordy. 2011. Inorganic carbon dynamics during northern California coastal upwelling. Cont. Shelf Res. **31**: 1180–1192. doi:10.1016/j.csr.2011.04.006

Feely, R. A., and others. 2016. Chemical and biological impacts of ocean acidification along the west coast of North America. Estuar. Coast. Shelf Sci. **183**: 260–270. doi:10.1016/j.ecss.2016.08.043

Frame, E. R., and E. J. Lessard. 2009. Does the Columbia River plume influence phytoplankton community structure along the Washington and Oregon coasts? J. Geophys. Res. Oceans **114**: 1–13. doi:10.1029/2008JC004999

Freeland, H. J., and K. L. Denman. 1982. A topographically controlled upwelling center off southern Vancouver Island. J. Mar. Res. **40**: 1069–1093.

Garrison, D. L., S. M. Conrad, P. P. Eilers, and E. M. Waldron. 1992. Confirmation of domoic acid production by *Pseudo-nitzschia australis* (Bacillariophyceae) cultures. J. Phycol. **28**: 604–607.

Gruber, N., C. Hauri, Z. Lachkar, D. Loher, T. L. Frölicher, and G. K. Plattner. 2012. Rapid progression of ocean acidification

in the California Current System. Science **337**: 220–223. doi:10.1126/science.1216773

Harvey, C. J., and others. 2020. Ecosystem status report of the California Current for 2019–20: A summary of ecosystem indicators compiled by the California Current Integrated Ecosystem Assessment Team (CCIEA). National Oceanographic & Atmospheric Administration Northwest Fisheries Science Center. doi:10.25923/e5rb-9f55

Harvey, C.J. and others. 2023. Ecosystem status report of the California Current for 2022–23: A summary of ecosystem indicators compiled by the California Current Integrated Ecosystem Assessment Team (CCIEA). National Oceanographic & Atmospheric Administration Northwest Fisheries Science Center.

Hauri, C., N. Gruber, G. K. Plattner, S. Alin, R. A. Feely, B. Hales, and P. A. Wheeler. 2009. Ocean acidification in the California Current System. Oceanography **22**: 60–71. doi:10.5670/oceanog.2009.97

Hickey, B. M., S. Geier, N. Kachel, and A. MacFadyen. 2005. A bi-directional river plume: The Columbia in summer. Cont. Shelf Res. **25**: 1631–1656. doi:10.1016/j.csr.2005.04.010

Hickey, B. M., and N. S. Banas. 2008. Why is the northern end of the California Current System so productive? Oceanography **21**: 90–107. doi:10.5670/oceanog.2008.07

Hickey, B. M., V. L. Trainer, P. M. Kosro, N. G. Adams, T. P. Connolly, N. B. Kachel, and S. L. Geier. 2013. A springtime source of toxic *Pseudo-nitzschia* cells on razor clam beaches in the Pacific Northwest. Harmful Algae **25**: 1–14. doi:10.1016/j.hal.2013.01.006

Hobday, A. J., and others. 2016. A hierarchical approach to defining marine heatwaves. Prog. Oceanogr. **141**: 227–238. doi:10.1016/j.pocean.2015.12.014

Hurst, C., Q. Dortch, G. Doucette, and M. Suddleson. 2020. Framework for the National Harmful Algal Bloom Observing Network: A workshop report. National Centers for Coastal Ocean Science and U.S. Integrated Ocean Observing System.

Hutchins, D. A., and F. Fu. 2017. Microorganisms and ocean global change. Nat. Microbiol. **2**: 17058. doi:10.1038/nmicrobiol.2017.58

Isles, P. D. 2020. The misuse of ratios in ecological stoichiometry. Ecology **101**: e03153.

Jacox, M. G., C. A. Edwards, E. L. Hazen, and S. J. Bograd. 2018. Coastal upwelling revisited: Ekman, Bakun, and improved upwelling indices for the US West Coast. J. Geophys. Res. Oceans **123**: 7332–7350. doi:10.1029/2018JC014187

Kadko, D. C., L. Washburn, and B. Jones. 1991. Evidence of subduction within cold filaments of the northern California coastal transition zone. J. Geophys. Res. Oceans **96**: 14909–14926. doi:10.1029/91JC00885

Kudela, R. M., J. Q. Lane, and W. P. Cochlan. 2008. The potential role of anthropogenically derived nitrogen in the growth of harmful algae in California, USA. Harmful Algae **8**: 103–110. doi:10.1016/j.hal.2008.08.019

Kudela, R. M., and T. D. Peterson. 2009. Influence of a buoyant river plume on phytoplankton nutrient dynamics: What controls standing stocks and productivity? J. Geophys. Res. Oceans **114**: 1–15. doi:10.1029/2008JC004913

Kudela, R. M., S. Seeyave, and W. P. Cochlan. 2010. The role of nutrients in regulation and promotion of harmful algal blooms in upwelling systems. Prog. Oceanogr. **85**: 122–135. doi:10.1016/j.pocean.2010.02.008

Lefebvre, K. A., M. Silver, S. Coale, and R. Tjeerdema. 2002. Domoic acid in planktivorous fish in relation to toxic *Pseudo-nitzschia* cell densities. Mar. Biol. **140**: 625–631. doi:10.1007/s00227-001-0713-5

Lundholm, N., P. J. Hansen, and Y. Kotaki. 2004. Effect of pH on growth and domoic acid production by potentially toxic diatoms of the genera *Pseudo-nitzschia* and *Nitzschia*. Mar. Ecol. Prog. Ser. **273**: 1–15. doi:10.3354/meps273001

MacFadyen, A., B. M. Hickey, and W. P. Cochlan. 2008. Influences of the Juan de Fuca Eddy on circulation, nutrients, and phytoplankton production in the northern California Current System. J. Geophys. Res. Oceans **113**: 1–19. doi:10.1029/2007JC004412

Maldonado, M. T., M. P. Hughes, E. L. Rue, and M. L. Wells. 2002. The effect of Fe and Cu on growth and domoic acid production by *Pseudo-nitzschia multiseries* and *Pseudo-nitzschia australis*. Limnol. Oceanogr. **47**: 515–526. doi:10.4319/lo.2002.47.2.0515

Mann, K. H. 2000. Ecology of coastal waters, with implications for management, 2nd ed. Blackwell Science.

McCabe, R. M., and others. 2016. An unprecedented coastwide toxic algal bloom linked to anomalous ocean conditions. Geophys. Res. Lett. **43**: 10–366. doi:10.1002/2016GL070023

McCabe, R. M., B. M. Hickey, and V. L. Trainer. 2023. The Pacific northwest harmful algal blooms bulletin. Harmful Algae **127**: 102480. doi:10.1016/j.hal.2023.102480

McKibben, S. M., W. Peterson, A. M. Wood, V. L. Trainer, M. Hunter, and A. E. White. 2017. Climatic regulation of the neurotoxin domoic acid. Proc. Natl. Acad. Sci. USA **114**: 239–244.

Moore, S. K., and others. 2021. An autonomous platform for near real-time surveillance of harmful algae and their toxins in dynamic coastal shelf environments. J. Mar. Sci. Eng. **9**: 336. doi:10.3390/jmse9030336

Olson, R. J., and H. M. Sosik. 2007. A submersible imaging-in-flow instrument to analyze nano-and microplankton: Imaging FlowCytobot. Limnol. Oceanogr. Methods **5**: 195–203. doi:10.4319/lom.2007.5.195

Pierrot, D., and others. 2009. Recommendations for autonomous underway pCO_2 measuring systems and data-reduction routines. Deep Sea Res. II Topic. Stud. Oceanogr. **56**: 512–522. doi:10.1016/j.dsr2.2008.12.005

Pozo Buil, M., and others. 2021. A dynamically downscaled ensemble of future projections for the California current system. Front. Mar. Sci. **8**: 612874. doi:10.3389/fmars.2021.612874

Preston, C., and others. 2024. Autonomous eDNA collection using an uncrewed surface vessel over a 4200-km transect of the eastern Pacific Ocean. Environ. DNA **6**: e468. doi:10.1002/edn3.468

Ryan, J. P., and others. 2017. Causality of an extreme harmful algal bloom in Monterey Bay, California, during the 2014–2016 northeast Pacific warm anomaly. Geophys. Res. Lett. **44**: 5571–5579. doi:10.1002/2017GL072637

Rykaczewski, R. R., J. P. Dunne, W. J. Sydeman, M. García-Reyes, B. A. Black, and S. J. Bograd. 2015. Poleward displacement of coastal upwelling-favorable winds in the ocean's eastern boundary currents through the 21st century. Geophys. Res. Lett. **42**: 6424–6431. doi:10.1002/2015GL064694

Sandoval-Belmar, M., and others. 2023. A cross-regional examination of patterns and environmental drivers of *Pseudo-nitzschia* harmful algal blooms along the California coast. Harmful Algae **126**: 102435. doi:10.1016/j.hal.2023.102435

Scannell, H. A., A. J. Pershing, M. A. Alexander, A. C. Thomas, and K. E. Mills. 2016. Frequency of marine heatwaves in the North Atlantic and North Pacific since 1950. Geophys. Res. Lett. **43**: 2069–2076. doi:10.1002/2015GL067308

Scholin, C., and others. 2009. Remote detection of marine microbes, small invertebrates, harmful algae, and biotoxins using the Environmental Sample Processor (ESP). Oceanography **22**: 158–167. http://www.jstor.org/stable/24860967

Small, L. F., and D. W. Menzies. 1981. Patterns of primary productivity and biomass in a coastal upwelling region. Deep Sea Res. A Oceanogr. Res. Pap. **28**: 23–149. doi:10.1016/0198-0149(81)90086-8

Smith, J., and others. 2018. A decade and a half of *Pseudo-nitzschia* spp. and domoic acid along the coast of southern California. Harmful Algae **79**: 87–104. doi:10.1016/j.hal.2018.07.007

Stone, H. B., N. S. Banas, P. MacCready, R. M. Kudela, and B. Ovall. 2020. Linking chlorophyll concentration and wind patterns using satellite data in the Central and Northern California Current System. Front. Mar. Sci. **7**: 551562. doi:10.3389/fmars.2020.551562

Sun, J., D. A. Hutchins, Y. Feng, E. L. Seubert, D. A. Caron, and F. X. Fu. 2011. Effects of changing pCO_2 and phosphate availability on domoic acid production and physiology of the marine harmful bloom diatom *Pseudo-nitzschia multiseries*. Limnol. Oceanogr. **56**: 829–840. doi:10.4319/lo.2011.56.3.0829

Tatters, A. O., F. X. Fu, and D. A. Hutchins. 2012. High CO_2 and silicate limitation synergistically increase the toxicity of *Pseudo-nitzschia fraudulenta*. PLoS One **7**: e32116. doi:10.1371/journal.pone.0032116

Thukral, M., and others. In press. High resolution biological and physical sampling reveals expression of domoic acid biosynthetic genes at frontal zones. *bioRxiv*. doi:10.1101/2023.10.19.562961

Todd, E. C. 1993. Domoic acid and amnesic shellfish poisoning—A review. J. Food Prot. **56**: 69–83. doi:10.4315/0362-028X-56.1.69

Trainer, V. L., N. G. Adams, B. D. Bill, C. M. Stehr, J. C. Wekell, P. Moeller, M. Busman, and D. Woodruff. 2000. Domoic acid production near California coastal upwelling zones, June 1998. Limnol. Oceanogr. **45**: 1818–1833. doi:10.4319/lo.2000.45.8.18182000

Trainer, V. L., and others. 2009. Variability of *Pseudo-nitzschia* and domoic acid in the Juan de Fuca eddy region and its adjacent shelves. Limnol. Oceanogr. **54**: 289–308. doi:10.4319/lo.2009.54.1.0289

Trainer, V. L., S. S. Bates, N. Lundholm, A. E. Thessen, W. P. Cochlan, N. G. Adams, and C. G. Trick. 2012. *Pseudo-nitzschia* physiological ecology, phylogeny, toxicity, monitoring and impacts on ecosystem health. Harmful Algae **14**: 271–300. doi:10.1016/j.hal.2011.10.025

Trainer, V. L., S. K. Moore, G. Hallegraeff, R. M. Kudela, A. Clement, J. I. Mardones, and W. P. Cochlan. 2020. Pelagic harmful algal blooms and climate change: Lessons from nature's experiments with extremes. Harmful Algae **91**: 101591. doi:10.1016/j.hal.2019.03.009

Wetz, M. S., and P. A. Wheeler. 2004. Response of bacteria to simulated upwelling phytoplankton blooms. Mar. Ecol. Prog. Ser. **272**: 49–57.

Wilkerson, F. P., and R. C. Dugdale. 1987. The use of large shipboard barrels and drifters to study the effects of coastal upwelling on phytoplankton dynamics. Limnol. Oceanogr. **32**: 368–382. doi:10.4319/lo.1987.32.2.0368

Wingert, C. J., and W. P. Cochlan. 2021. Effects of ocean acidification on the growth, photosynthetic performance, and domoic acid production of the diatom *Pseudo-nitzschia australis* from the California Current System. Harmful Algae **107**: 102030. doi:10.1016/j.hal.2021.102030

Acknowledgments

Special thanks to Ethan Beyer, Alicia Billings, Julia Clemons, Sandy Parker-Stetter, and the rest of the scientific team, officers, and crew aboard the NOAA Ship *Bell M. Shimada* for collecting samples and assisting in the operations and maintenance of the IFCB and pCO_2 system. We also thank Vera Trainer and Nick Adams for collecting particulate DA and nutrient data; Jan Newton and Terrie Klinger for helpful discussions; Tom Fougere, Vinny Ferreira, and Ivory Engstrom for assistance with IFCB troubleshooting; Kendra Hayashi for preparing an IFCB for cruise-deployment; Kelly George for annotating IFCB images from the Oregon coast; Andrew Leising for advice on marine heatwaves; and Jennifer Fisher for providing Newport Hydrographic Line data. A.D.F. was supported by a Washington Ocean Acidification Center award, which was administered by UCAR's Cooperative Programs for the Advancement of Earth System Science under contract #61878. The 2019 IFCB deployment was supported by a NOAA Northwest Fisheries Science Center Internal Grant Program award to S.K.M. The 2021 IFCB deployment was partially supported by NOAA award NA21NOS0120090 to R.M.K. and National Aeronautics and Space Administration award 80NSSC20M0008 to M.T.K. Sustained underway pCO_2 observations were funded by NOAA Ocean Acidification Program (NRDD 20845 and 20847) grants to S.R.A. and A.U.C. This is PMEL contribution #5560. This publication was

partially funded by the Cooperative Institute for Climate, Ocean, and Ecosystem Studies under NOAA Cooperative Agreement NA20OAR4320271, contribution #2023-1318.

Conflict of Interest

The authors have no conflicts of interest to declare.

Submitted 14 December 2023
Revised 22 March 2024
Accepted 27 May 2024

Associate editor: Bingzhang Chen